International Journal of Thermophysics, Vol. 28, No. 4, August 2007 (© 2007)
DOI: 10.1007/s10765-007-0202-2

Numerical Analysis of Convective Instabilities in a Transient Short-Hot-Wire Setup for Measurement of Liquid Thermal Conductivity

Roberto Rusconi,[1,2] Wesley C. Williams,[1] Jacopo Buongiorno,[1] Roberto Piazza,[2] and Lin-Wen Hu[1,3]

Received January 16, 2007

Numerical simulation has been used to investigate the effects of natural convection on measurements of the thermal conductivity of fluids by transient hot-wire methods. Comparison of the numerical data with the experimental results obtained with a custom-built setup exploiting a short-wire geometry allows fixing an operationally useful time scale, where convective effects can be safely neglected.

KEY WORDS: convection; liquids; numerical simulations; thermal conductivity; transient hot-wire technique.

1. INTRODUCTION

Obtaining accurate and reliable values for the thermal conductivity of pure liquids or fluid mixtures is a primary need for many applications, for instance, fast and efficient removal of excess heat from solid surfaces in thermal management systems. A crucial issue in the design of experimental techniques is to reduce as much as possible any spurious convective effect that, due to the generally much stronger contribution of advection to thermal transport, noticeably affects thermal-conductivity measurements. Quite often, however, the occurrence of weak horizontal temperature gradients,

[1]Massachusetts Institute of Technology, 77 Massachusetts Avenue, Cambridge, Massachusetts, 02139, U.S.A.
[2]Dipartimento di Ingegneria Nucleare, Politecnico di Milano, via Ponzio 34/3, Milano 20133, Italy.
[3]To whom correspondence should be addressed. E-mail: lwhu@mit.edu

which triggers natural convection, is unavoidable in practical setups. A popular remedial strategy consists in performing measurements on a time scale short enough that advective transport can be safely neglected. Such a strategy is, for instance, exploited in the transient hot-wire (THW) technique [1–6], which in the last two decades has become the 'benchmark' method for thermal-conductivity measurements in fluids.

Recently, Zhang et al. [7,8] have proposed and successfully tested an improved THW method exploiting a very short probing wire, which permits minimizing the sample volume and the overall setup size. This is important in applications to electrically conducting or highly corrosive fluids, such as molten salts, where substantial wire insulation is imperative and homogeneous sample thermalization is hard to maintain. Unfortunately, the standard analytical treatment valid for an infinitely long heat source is no longer applicable to short wires, and computational analysis is required both for deriving the time evolution of the temperature field and, even more, to properly quantify natural convection effects. The main objective of this paper is presenting and discussing numerical simulations of heat conduction and convective instabilities in a transient short-hot-wire geometry, and comparing them with experimental data for liquids such as water and ethylene glycol (EG) obtained with a setup developed in our labs.

2. STATEMENT OF THE PROBLEM

The THW method consists of applying a constant current to a conducting wire with a typical radius $a \lesssim 15\,\mu\text{m}$, usually made of platinum or tantalum, and measuring the time dependence of its electrical resistance, which is directly proportional to the wire temperature. Therefore, the wire acts at the same time as a heat source and a probe. For measurements in electrically conducting liquids, the wire must obviously be coated by a thin insulation layer. Provided that some simplifying approximation are made, the thermal conductivity of the medium can be analytically related to the temperature increase ΔT of the wire. Indeed, assuming that:

(a) the wire is infinitely long, has a thermal conductivity much larger than the fluid, and a negligible heat capacity;

(b) the power q dissipated per unit length is constant; and

(c) the fluid is incompressible and has temperature-independent thermal conductivity λ and diffusivity κ within the range of measurement;

one simply obtains a time-dependent temperature increase

$$\Delta T(t) = \frac{q}{4\pi\lambda} E_1\left(\frac{a^2}{4\kappa t}\right), \tag{1}$$

where $E_1(x)$ is the exponential integral function. Provided that $t \gg a^2/4\kappa$ (which, for ordinary fluids, means t larger than a few milliseconds), the transient temperature rise can be further approximated as

$$\Delta T \simeq \frac{q}{4\pi\lambda}\left[\ln(t) + \ln\left(\frac{4\kappa}{a^2 C}\right)\right], \tag{2}$$

where $C = \exp(\gamma) \simeq 1.781$ and γ is the Euler constant. Therefore, the slope and intercept of the ΔT versus $\ln(t)$ curve can be used to simultaneously measure λ and κ. In practice, however, the experimental uncertainty for the thermal diffusivity is usually almost an order of magnitude larger than for the thermal conductivity [9].

A rigorous, albeit slightly more elaborated, analytical solution can still be obtained even assuming a finite thermal conductivity λ_w and heat capacity $(\rho c_p)_w$ of the wire [1]:

$$\Delta T \simeq \frac{q}{4\pi\lambda}\left\{\left[1 - \frac{(\rho c_p)_w - (\rho c_p)}{2\lambda t} a\right]\ln\left(\frac{4\kappa t}{a^2 C}\right) + \frac{a^2}{2\kappa t} - \frac{a^2}{4\kappa_w t} + \frac{\lambda}{2\lambda_w}\right\} \tag{3}$$

where κ_w is the thermal diffusivity of the wire. Due to the high value of thermal conductivity and the small size of the wire, these corrections are significant only for the long-time behavior of the THW signal. The latter is also modified by the finite size of the vessel containing the investigated sample, setting the heat flux and temperature increase at the boundaries. For a cylindrical vessel of radius b, the maximal steady-state temperature increase is [1]

$$\Delta T_\infty = \frac{q}{2\pi\lambda}\ln(b/a). \tag{4}$$

Finite size effects are however significant only for $t \gtrsim b^2/2\kappa$ [9], which, for b of the order of 1 cm, is typically for liquids in the hundreds of seconds range. One should also take into account that, since the wire resistance depends on temperature, the dissipated electrical power actually depends on time. Yet, for small temperature increments, this effect can be safely neglected. For a short wire with a length-to-radius ratio $L/a \lesssim 10^3$, a further correction based on the axial conduction of the wire can be analytically modeled as shown in Ref. 10, particularly for $\lambda_w \gg \lambda$.

A crucial assumption underlying the analytical approaches described above is that the fluid is at rest, i.e., that convective effects, carrying heat away advectively and therefore reducing the wire-temperature increase, can be neglected. Natural convection is however intrinsically unavoidable, due to the presence of the horizontal component of the temperature gradient brought forth by the cylindrical geometry of the wire.

Convection effects will be stronger the larger is the vertical extent of the sample, ℓ, which is obviously constrained by the wire length. Assuming small temperature increments, neglecting inertial forces, and equating viscous forces to buoyancy, a characteristic value for the fluid convection velocity is given by $U \sim g\alpha\ell^2\Delta T/\nu$, where ν and α are the kinematic viscosity and thermal expansion coefficient of the fluid, respectively, and g is the acceleration of gravity [11]. This estimate is, however, valid only for very short wires and low dissipation. By increasing the wire length or the applied power, inertial forces become indeed dominant with respect to viscous terms, yielding a characteristic fluid velocity scaling as ℓ as $U \sim (g\alpha\Delta T\ell)^{1/2}$. As a first approximation, THW measurements will be meaningful only provided they last for a time $t \ll \ell/\mathrm{U}$. These assumptions can be checked by solving the conservation equations for momentum and energy, and the only way is by resorting to numerical simulation.

3. NUMERICAL SIMULATIONS

Numerical simulations have been performed using a finite element method (FEM) routine, *FlexPDE* (PDE Solutions Inc.), which requires a direct implementation of the governing equations. By exploiting the symmetry of the problem, we selected a two-dimensional cylindrical model with a self-adapting mesh of about 15,000 triangular elements (Fig. 1). The temporal dependence of the temperature field is integrated using a second-order implicit method.

In the fluid region, the equations used in the simulations are the Navier-Stokes equations in the Boussinesq approximation, the so-called "Poisson pressure" equation and the heat diffusion equation:

$$\nu\nabla\cdot\nabla v_r = \frac{1}{\rho}\frac{\partial p}{\partial r} + v_r\frac{\partial v_r}{\partial r} + v_z\frac{\partial v_r}{\partial z} + \frac{\partial v_r}{\partial t} \tag{5}$$

$$\nu\nabla\cdot\nabla v_z = \frac{1}{\rho}\frac{\partial p}{\partial r} + v_r\frac{\partial v_z}{\partial r} + v_z\frac{\partial v_z}{\partial z} + \frac{\partial v_z}{\partial t} - g\alpha\Delta T \tag{6}$$

$$\nabla\cdot\nabla(p/\rho) = \delta\left[\frac{1}{r}\frac{\partial(rv_r)}{\partial r} + \frac{\partial v_z}{\partial z}\right] + 2\left(\frac{\partial v_r}{\partial r}\frac{\partial v_z}{\partial z} - \frac{\partial v_r}{\partial z}\frac{\partial v_z}{\partial r}\right) + g\alpha\frac{\partial\Delta T}{\partial z} \tag{7}$$

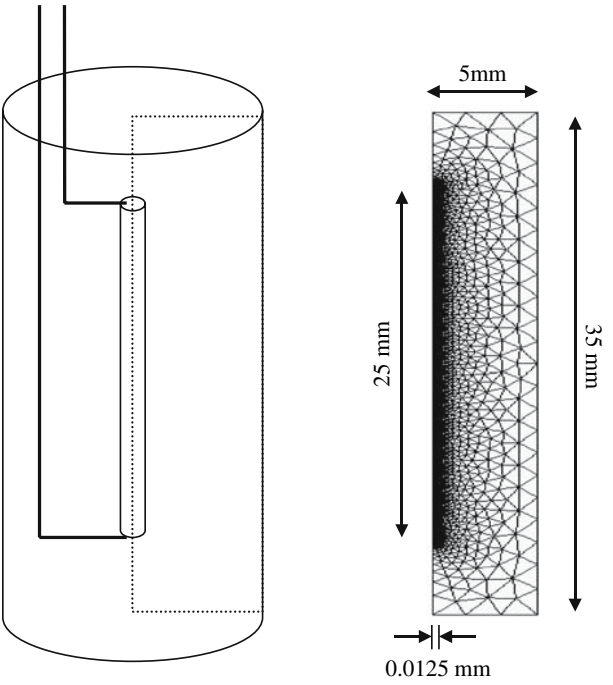

Fig. 1. Computational domain used in numerical simulations.

$$\kappa \nabla \cdot \nabla(\Delta T) = v_r \frac{\partial \Delta T}{\partial r} + v_z \frac{\partial \Delta T}{\partial z} + \frac{\partial \Delta T}{\partial t} \tag{8}$$

where v_r and v_z are, respectively, the radial and axial components of the fluid velocity, ρ is the fluid density, and δ is an appropriate penalty coefficient, which numerically enforces the incompressibility of the velocity field (for further details, see Ref. 11). Within the solid wire, only the heat transport equation (with the source term) is integrated.

3.1. Numerical Analysis of the Heat-Conduction Model

To compare the simulations to the experimental results, the numerical analysis of the heat diffusion equation was performed for both a tantalum and a platinum wire immersed in water. We also considered the effects of a thin insulation layer with a thickness of $1.5\,\mu\mathrm{m}$ around a platinum wire. Assumed values for ρ, λ and c_p are, respectively, $16.69\,\mathrm{g \cdot cm^{-3}}$, $57.5\,\mathrm{W \cdot m^{-1} \cdot K^{-1}}$, and $0.14\,\mathrm{J \cdot g^{-1} \cdot K^{-1}}$ for tantalum; $21.45\,\mathrm{g \cdot cm^{-3}}$, $71.6\,\mathrm{W \cdot m^{-1} \cdot K^{-1}}$, and $0.13\,\mathrm{J \cdot g^{-1} \cdot K^{-1}}$ for platinum;

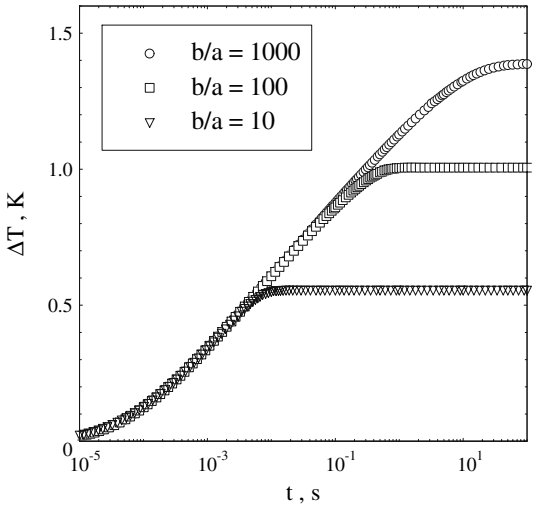

Fig. 2. Numerical analysis of the heat-conduction equation ($g = 0$ is assumed) for different values of the vessel-to-wire radius.

and $1.4\,\mathrm{g \cdot cm^{-3}}$, $0.2\,\mathrm{W \cdot m^{-1} \cdot K^{-1}}$, and $1\,\mathrm{J \cdot g^{-1} \cdot K^{-1}}$ for the coating. The physical properties and the thickness of the insulation layer are such that it does not significantly alter the temperature rise of the wire.

Before discussing the convective effects, we shall compare the simulation results with some basic features of the THW method discussed in the previous section. Figure 2 shows the wire volume-averaged temperature rise ΔT for three different values of the ratio b/a between vessel and wire radii. Consistent with Eq. (4), the steady-state value is found to be proportional to $\ln(b/a)$. Figure 3 displays the results obtained for different lengths of the wire. For $L = 25\,\mathrm{mm}$, the thermal conductivity is found to be $\lambda = 0.621\,\mathrm{W \cdot m^{-1} \cdot K^{-1}}$, which is only slightly larger than the actual value for water $\lambda = 0.607\,\mathrm{W \cdot m^{-1} \cdot K^{-1}}$. Note however that, for sufficiently long time, the discrepancies with the theoretical model become quite large for shorter wires. Conversely, the inset confirms that the ratio between temperature rise and dissipated power does not depend on the input current.

3.2. Convective Effects

We first analyzed the effect of the numerical parameters used in the simulation (mesh size, solution controls, and penalty factor) on the

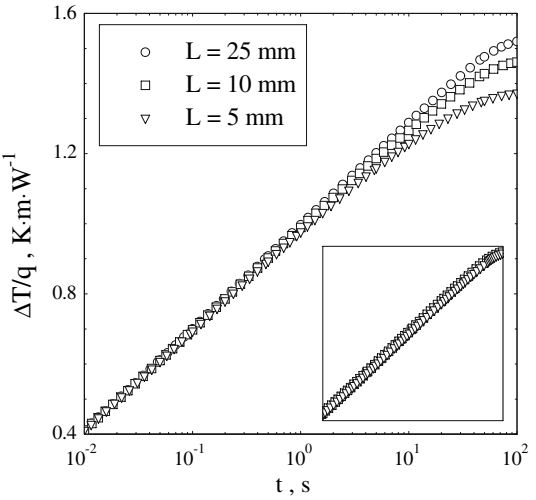

Fig. 3. Numerical analysis of the heat-conduction equation for different wire lengths. Inset: normalized temperature versus time for an applied current $I = 50\,\text{mA}$ (circles), $I = 100\,\text{mA}$ (squares), and $I = 500\,\text{mA}$ (triangles).

accuracy of the solution. Figure 4 shows the results for the thermal and velocity field for a tantalum wire at $t = 100\,\text{s}$ with an applied current $I = 100\,\text{mA}$. Comparison of the temperature profiles in the presence and in the absence of natural convection (the latter obtained by setting $g = 0$), shown to the left side of the figure, clearly shows that convective rolls (with a velocity field displayed in the last panel to the right) do modify the thermal distribution all along the wire. Figure 5, displaying the time dependence of the volume-averaged temperature increase $< \Delta T >$, shows that deviations from the convection-free solution start to be appreciable after a few seconds, reaching about 2% for $t = 10\,\text{s}$. However, the most striking effect is that the temperature field along the wire becomes strongly non-uniform, as highlighted by the temperature variations at two locations symmetric with respect to the wire midplane which, in the absence of convection, should be at the same temperature. Note that this temperature difference is already pronounced after 1 s, so that the lesser sensitive to convection of $< \Delta T >$ comes only from compensation associated to averaging.

Figure 6, where we compare the numerical results obtained for different values of the applied current, shows that, by increasing the dissipated power, the normalized temperature starts deviating from a logarithmic

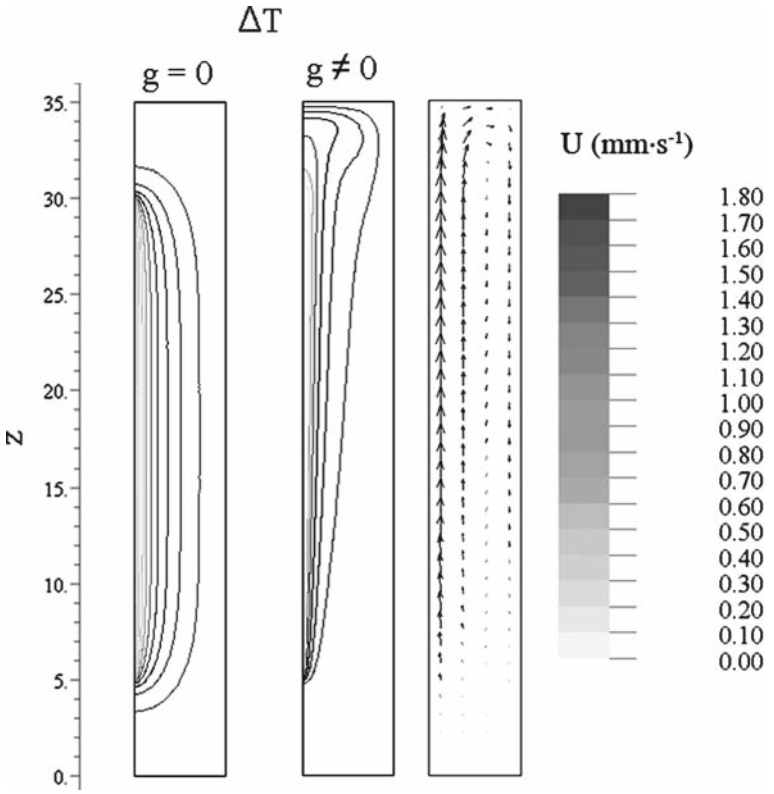

Fig. 4. Numerical results for the thermal and velocity field after 100 s in a tantalum wire with an applied current $I = 100\,\text{mA}$.

growth earlier, due to the stronger role played by convection. For instance, comparing the data obtained for $I = 50$ and 250 mA, the time t^* it takes to observe a deviation of more than 1% (conventionally assumed as an 'operational onset time' for convection) reduces by about one order of magnitude. Furthermore, since the viscosity of fluids (and water in particular) decreases with temperature, convective effects are stronger at higher average sample temperature. This is clearly highlighted by Fig. 7, where results for water at 25 and 75°C are compared, together with the corresponding velocity fields in the inset. In practical applications, the electrical current used in THW measurements typically ranges between 50 and 100 mA, and quite often measurements performed at different outer temperatures must be compared. Careful assessment of the build-up time of natural convection effects is therefore crucial.

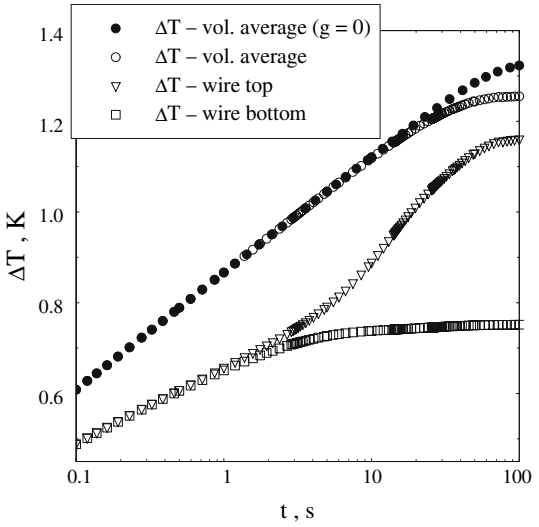

Fig. 5. Numerical results for the temperature increments in a tantalum wire with an applied current $I = 100$ mA.

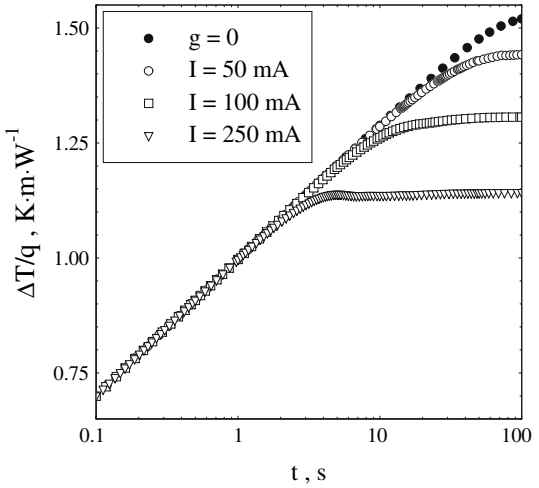

Fig. 6. Numerical results for different applied currents.

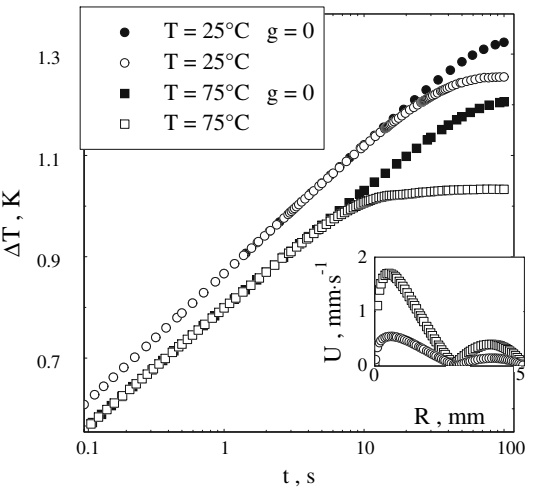

Fig. 7. Numerical results for the temperature rise at 25 and 75°C. Inset: magnitude of the velocity field at the wire midplane.

Finally, Fig. 8 displays the dependence on wire length of t^*, evaluated either from the corresponding maximum convective velocity (shown in the inset) or directly from simulation. As theoretically predicted in the case of non-negligible inertial forces, the dependence of the characteristic velocity with the vertical extent is roughly $L^{1/2}$. Yet, the numerical onset times display a more linear behavior than the calculated ones. For future work, it would be of interest to consider the spurious effects associated with a non-vertical setting of the wire. Since this could not be modeled in cylindrical symmetry, the analysis would require a more complex, three-dimensional simulation.

4. EXPERMENTIAL SETUP

To test the simulation results presented in Section 3, we have designed and built a short-wire THW setup, which is schematically drawn in Fig. 9. We have used both a non-insulated tantalum wire, with a diameter of 25 μm and a platinum wire with Isonel coating and a core diameter of 25 μm (28 μm including the insulating coating). In both cases, the wire length is about 2.5 cm. Two electrically insulated tantalum rods are used both as supporting leads keeping the wire in tension and as electrical connections. The input current is provided by a precision tunable source (Keithley, Model 6221). Since changes of the wire resistance typically

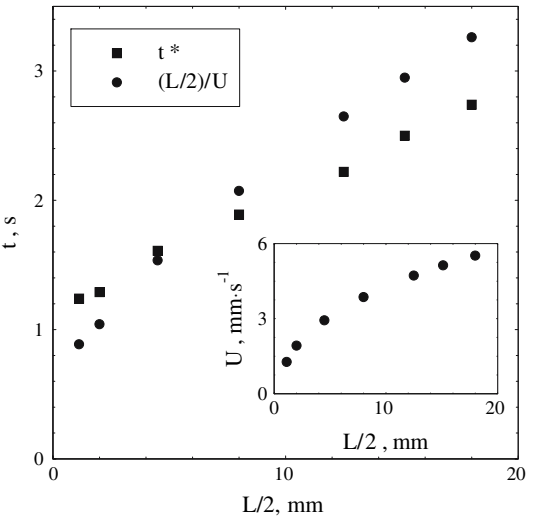

Fig. 8. Onset time and maximum velocity (inset) as a function of the half-length of the wire. Applied current has been chosen to keep the dissipated power per unit length q constant.

yield voltage signals $\Delta V < 1\,\text{mV}$, a high-sensitivity nanovoltmeter (Keithley, Model 2182A) is used for detection. The sample is contained in a stainless steel vessel with a diameter of about 2.5 cm, accommodated in a constant-temperature container. The current source and the voltmeter are remotely controlled through a GPIB interface using custom-made software. The simulation results suggest that the acquisition rate has to be sufficiently high to ensure the collection of a large number of data points before convection effects set in. In our measurements, an acquisition rate of about $60\,\text{s}^{-1}$ was found to be adequate. The total measurement time is set to 20 s. For the first 5 s the system acquires the voltage signal at very low input current (usually 1 mA), to obtain the wire resistance before heating, which also yields the actual sample temperature via the known resistance–temperature relation for the wire. Then, the input current is raised to a much higher value and the transient voltage signal is acquired and transferred to the controlling PC. To test the dependence of convective effects on the dissipated power, a series of runs is performed and averaged for different values of the input current up to a maximum value of 100 mA.

By direct calibration, the temperature dependence of both wires was found to be linear in the range of 10–50°C with a coefficient of $0.0037\,\Omega \cdot K^{-1}$ for platinum and $0.0028\,\Omega \cdot K^{-1}$ for tantalum, which are quite close

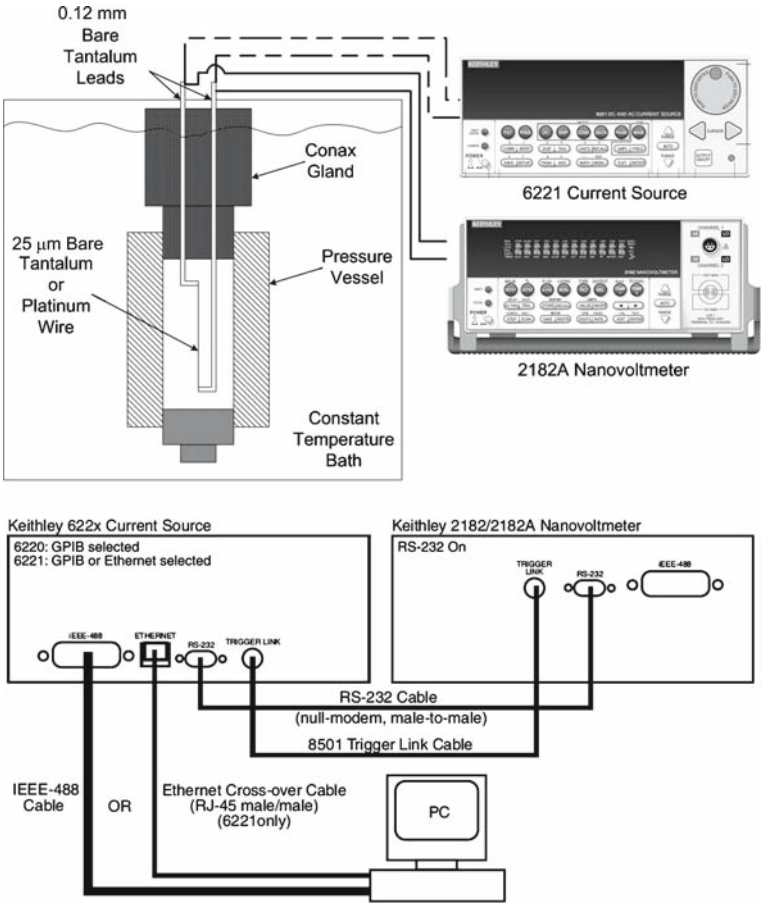

Fig. 9. Schematic of transient hot-wire setup.

to the tabulated values ($0.0039\,\Omega \cdot K^{-1}$ and $0.0036\,\Omega \cdot K^{-1}$, respectively). The length of the wire, determined using the thermal conductivity of water as a calibration factor, is quite close to the value measured with a caliper.

5. COMPARISON WITH SIMULATION

In Fig. 10 we compare experimental results and numerical simulations data for distilled water at 25 and 50°C for $I = 100\,\text{mA}$. As predicted, the experimental data shows a clear logarithmic trend over almost all the investigated time range, although a time-independent shift to higher ΔT values is observed. This shift does not affect the measurements of the

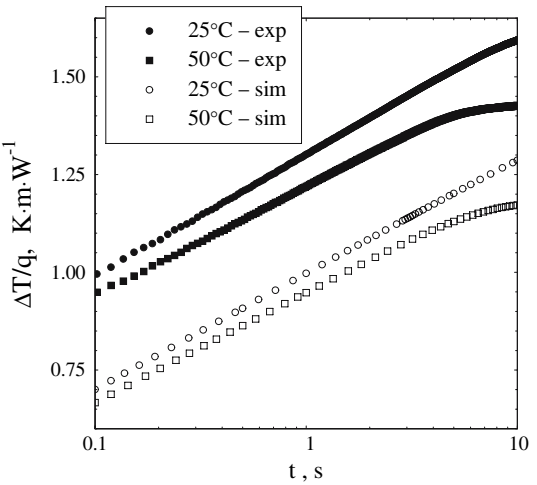

Fig. 10. Comparison between the experimental data and numerical simulations at 25 and 50°C for $I = 100\,\text{mA}$.

thermal conductivity, which depends on the slope of the ΔT versus $\ln(t)$ curve only. Interestingly, the agreement between experimental and numerical results for what concerns the temperature dependence of convective effects is quite good. That is, deviations from a simple logarithmic trend at long time are indeed found to be much more pronounced at 50°C than at 25°C, with an evident temporal correlation between simulation and measurements. The presence of natural convection is clearly visible in Fig. 11 where experimental results for different applied currents (50, 70, and 100 mA) at 60°C are shown. In this case, the linear part (on a logarithmic scale) appears to be slightly affected by advective effects; consequently, the measured value of thermal conductivity will be somewhat different for different power levels, but always higher than the real value. Multi-current measurements are therefore a fundamental tool for careful control and detection of natural convection. As a further check of the reliability of our setup, we shown in the inset the measured value for the thermal conductivity of ethylene glycol (EG) in comparison with water. Due to the high viscosity of EG, measurements are essentially unaffected by convection, yielding a thermal conductivity $\lambda = 0.265\,\text{W}\cdot\text{m}^{-1}\cdot\text{K}^{-1}$ that is in close agreement with the value reported in literature ($0.257\,\text{W}\cdot\text{m}^{-1}\cdot\text{K}^{-1}$).

Finally in Fig. 12 the experimental data of thermal conductivity for water are displayed at different temperatures. The values have been obtained from a fit of the logarithmic part in the temporal window

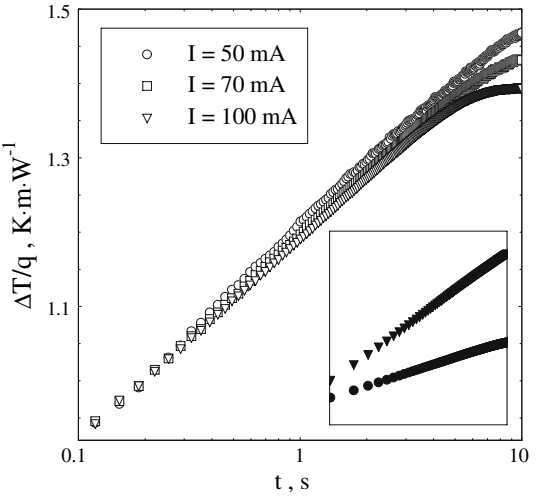

Fig. 11. Experimental results for different applied currents at 60°C. Inset: comparison between the experimental results for EG (triangles) and distilled water (circles).

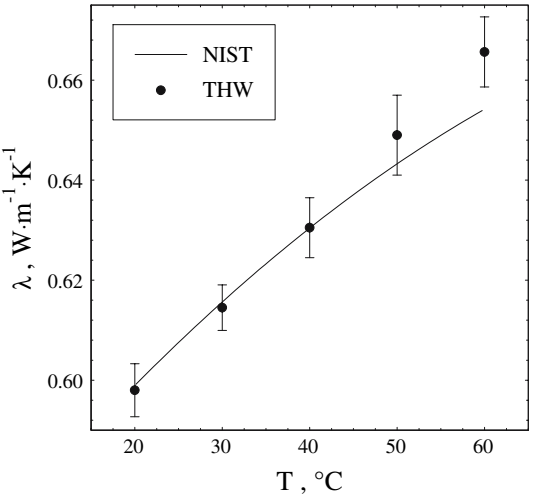

Fig. 12. Experimental data for the thermal conductivity of water at different temperatures. Error bars are the standard deviations of measurements performed at different current levels.

between 0.2 and 2 s, averaged over different powers. Agreement with literature values is quite good up to $T \simeq 40°C$, while again, for higher temperatures, the experimental data start to be affected by the presence of natural convection, yielding higher apparent values.

6. CONCLUSIONS

We have shown that computational analysis gives physical insight on the effects of natural convection on THW measurements, allowing quantitative determination of an operational time window where these effects can be safely neglected. Such a time window depends on the dissipated power as well as the physical properties of the investigated fluids. In particular, special care should be exercised when operating at high temperature, where inertial effects are more relevant. Provided that natural convection effects are carefully taken into account, the transient short-hot-wire method proves to be effective for measuring the thermal conductivity of liquids, yielding results which are in good agreement with standard data. The investigation we have performed may be of specific interest in the analysis of the thermal properties of nanofluids, i.e., colloidal dispersions of particles in the nanometer size range. These systems have recently attracted the attention of the scientific and engineering community due to some very unusual properties they seem to display when used as thermovector fluids, e.g., their ability to increase the convective heat transfer in flow experiments. These effects have been tentatively attributed to an anomalous thermal conductivity increase of the continuous phase brought on by the dispersed particles, but this explanation is still controversial both theoretically and experimentally. Our results leads us to conclude that the THW method, in particular, the short-wire configuration, in combination with computational modeling may shed light on these alleged thermal anomalies of nanofluids.

ACKNOWLEDGMENTS

This work was made possible by the generous support of the joint MIT/Politecnico "Progetto Rocca" Program, the Idaho National Laboratory, and the U.S. Department of Energy Innovations in Nuclear Infrastructure and Education grant.

REFERENCES

1. J. J. Healy, J. J. de Groot, and J. Kestin, *Physica* **82C**:392 (1976).

2. Y. Nagasaka and A. Nagashima, *J. Phys. E: Sci. Instrum*. **14**:1435 (1981).
3. H. M. Roder, *J. Res. Natl. Bur. Stand. (US)* **86**:457 (1981).
4. W. A. Wakeham, J. V. Sengers, and A. Nagashima, *Measurements of the Transport Properties of Fluids; Experimental Thermodynamics* (Blackwell Scientific, Oxford, 1991), Chap. 7, pp. 162–194.
5. M. J. Assael, L. Karagiannidis, N. Malamataris, and W. A. Wakeham, *Int. J. Thermophys*. **19**:379 (1998).
6. M. Khayet and J. M. Ortiz de Zarate, *Int. J. Thermophys*. **26**:637 (2005).
7. X. Zhang and M. Fujii, *Int. J. Thermophys*. **21**:71 (2000).
8. X. Zhang, W. Hendro, M. Fujii, T. Tomimura, and N. Imaishi, *Int. J. Thermophys*. **23**:1077 (2002).
9. U. Hammerschmidt and W. Sabuga, *Int. J. Thermophys*. **21**:1255 (2000).
10. W. T. Kierkus, N. Mani, and J. E. S. Venart, *Can. J. Phys*. **51**:1182 (1973).
11. R. Rusconi, L. Isa, and R. Piazza, *J. Opt. Soc. Am. B* **21**:605 (2004).